JOURNAL OF GEOPHYSICAL RESEARCH, VOL. 104, NO. D4, PAGES 4241–4248, FEBRUARY 27, 1999

Comment on "Contribution of different aerosol species to the global aerosol extinction optical thickness: Estimates from model results" by Tegen et al.

Patricia K. Quinn and Derek J. Coffman

Pacific Marine Environmental Laboratory, NOAA, Seattle, Washington
Joint Institute for the Study of the Atmosphere and Ocean, University of Washington, Seattle

1. Introduction

In their work, *Tegen et al.* [1997] approximate a global distribution of aerosol chemical composition by combining the output from several transport models [*Tegen and Fung,* 1995; *Chin et al.,* 1996; *Liousse et al.,* 1996]. The resulting distributions of soil dust, sea salt, sulfate, and carbonaceous aerosols then are used to estimate a global distribution of the aerosol optical thickness due to each component. The model results indicate that the extinction due to sea salt is small on both global and regional scales. In high-latitude regions of the southern hemisphere (80°S to 40°S), the maximum contribution of sea salt to total aerosol extinction is estimated to be 21 to 27%. In the tropics and middle to high-latitude regions of the northern hemisphere (20°S to 60°N), its contribution is estimated to be considerably lower at 10 to 15%. The model calculations assume a minimum diameter for sea-salt aerosol of 4 μm which, as the authors acknowledge, may lead to an underestimation of its optical depth.

In their introduction, *Tegen et al.* [1997] state that "Global transport models that are validated by ground-based measurements can provide a first estimate of global aerosol distributions in space and time." It is in this spirit that we offer here a review of recently published shipboard observations of sea-salt mass concentrations for a large portion of the Pacific and Southern Oceans. Size distributions of sea salt in the remote marine boundary layer, the contribution of sea salt to scattering by the aerosol, and mass-scattering efficiencies for submicron and supermicron sea salt are presented. These data show that sea salt can comprise a significant mass fraction of both submicron and supermicron aerosol, and scattering due to sea salt often dominates that of other major chemical components. Finally, optical depths of sea salt for a well-mixed boundary layer are estimated and compared to the results of *Tegen et al.* [1997].

2. Measurements

Chemical mass size distributions of sodium and sulfate were measured on several cruises in the Pacific and Southern Oceans using seven-stage Berner-type cascade impactors with subsequent chemical analysis by ion chromatography. Sea-salt concentrations were calculated from measured Na^+ concentrations and an average ionic composition of seawater [*Holland,* 1978]. Non-sea-salt sulfate (nss $SO_4^=$) concentrations were calculated from measured Na^+ concentrations and the $SO_4^=$ to Na^+ ratio in seawater [*Holland,* 1978]. The results of these measurements have been reported previously [*Quinn et al.,* 1995, 1996, 1998; *Quinn and Coffman,* 1998]. The PSI (Pacific Sulfur/Stratus Investigation) 91 cruise took place in April and May 1991 off the coast of Washington State. MAGE (Marine Aerosol and Gas Exchange cruise) 92 was conducted in February and March 1992 along 140°W from 33°N to 12°S. The RITS (radiatively important trace species) 93 cruise took place from March to May 1993 along 140°W from 70°S to 55°N, while RITS 94 was a reverse of this track in November and December 1993. Finally, ACE 1 (Aerosol Characterization Experiment) took place in November and December of 1995 in the Southern Ocean southwest of Tasmania. The data are collated and summarized here to provide validation of sea-salt distributions produced from global transport models and, in particular, the model of *Tegen et al.* [1997].

All chemical mass size distributions were measured at a low-reference relative humidity (RH) of 30 to 40% to ensure uniform size cuts under conditions of variable ambient humidity. We have adjusted the particle diameters to an RH of 70% by assuming uniform growth factors for all particle sizes of 1.3 and 1.5 for nss $SO_4^=$ (assuming a composition of NH_4HSO_4) and sea-salt aerosol, respectively. These values are based on calculations of *Tang* [1996], measurements of aerosol hygroscopic growth during ACE 1 [*Berg et al.,* 1998], and the assumptions that the sampled particles are externally mixed and do not completely dry out as they pass through the sampling inlet.

3. Sea-Salt Size Distributions

On the basis of mass closure experiments performed in the Pacific and Southern Oceans [*McInnes et al.,* 1996; *Quinn and Coffman,* 1998], the dominant chemical components in the remote marine boundary layer (MBL) are sea salt and nss $SO_4^=$. The scattering due

Paper number 1998JD200066.
0148-0227/99/1998JD200066$09.00

to each component depends on its size-dependent mass concentration. On a mass basis at a wavelength of 0.55 μm, the scattering efficiency of spherical particles is lognormally distributed with the most efficient size range for scattering occurring between particle diameters of about 0.2 and 1.0 μm [*Quinn et al.*, 1996]. Non-sea-salt $SO_4^=$ aerosol resides primarily within accumulation mode particles which have diameters between 0.06 and 1.0 μm. Therefore it can be an important component of the scattering by the aerosol. The majority of the sea-salt mass occurs in the coarse mode with diameters larger than 1.0 μm such that it lies outside of this optically active size range. Yet it is an important contributor to scattering by the aerosol for three reasons. First, the mass concentration of the supermicron or coarse mode sea salt is sufficient to compensate for the low-scattering efficiency of this size range. Second, given a large enough concentration, a considerable amount of coarse mode sea-salt mass can "tail" into the optically active size range. In addition, there is evidence of a mode of sea-salt aerosol within the submicron size range which is produced independently from coarse mode sea salt [*O'Dowd et al.*, 1997]. As a result, neglecting submicron sea salt will lead to an underestimation of the scattering due to this aerosol chemical component, especially in light of the relatively longer lifetime of aerosol within this size range.

Average sea-salt mass size distributions measured during each of the five cruises are shown in Figure 1. Also shown for comparison are the average nss $SO_4^=$ concentrations measured in each impactor size bin. The long latitudinal transects of RITS 93 and 94 have been segregated into the latitudinal bins considered by *Tegen et al.* [1997]. In all cases the average sea-salt size distribution indicates the presence of sea salt in submicron particles. In addition, the mass concentration of this submicron sea salt often is equal to or greater than that of nss $SO_4^=$.

The average and standard deviation of sea salt and nss $SO_4^=$ measured in two different size ranges ($D \leq 1.4$ μm and $1.4 < D < 10$ μm, where D is the geometric mass diameter at 70% RH) are shown in Table 1. The upper size limit of $\sim$10 μm is determined by the large-particle collection efficiency of the aerosol inlet. As a result, concentrations in the larger size range represent a lower bound of ambient supermicron sea-salt concentrations. This makes a direct comparison to the values of *Tegen et al.* [1997], which are only in the supermicron size range and have a minimum diameter of 4 μm, difficult. Given the different size ranges considered by the measurements and model, our goal cannot be to compare measured and modeled total sea-salt concentrations but rather to point out the extent to which sea salt occurs in the submicron size range and the effect this has on scattering by sea salt.

In open ocean regions, sea-salt concentrations in particles with $D \leq 1.4$ μm are relatively constant (0.79 $\pm$ 0.14 μg m^{-3}) and higher than those measured in

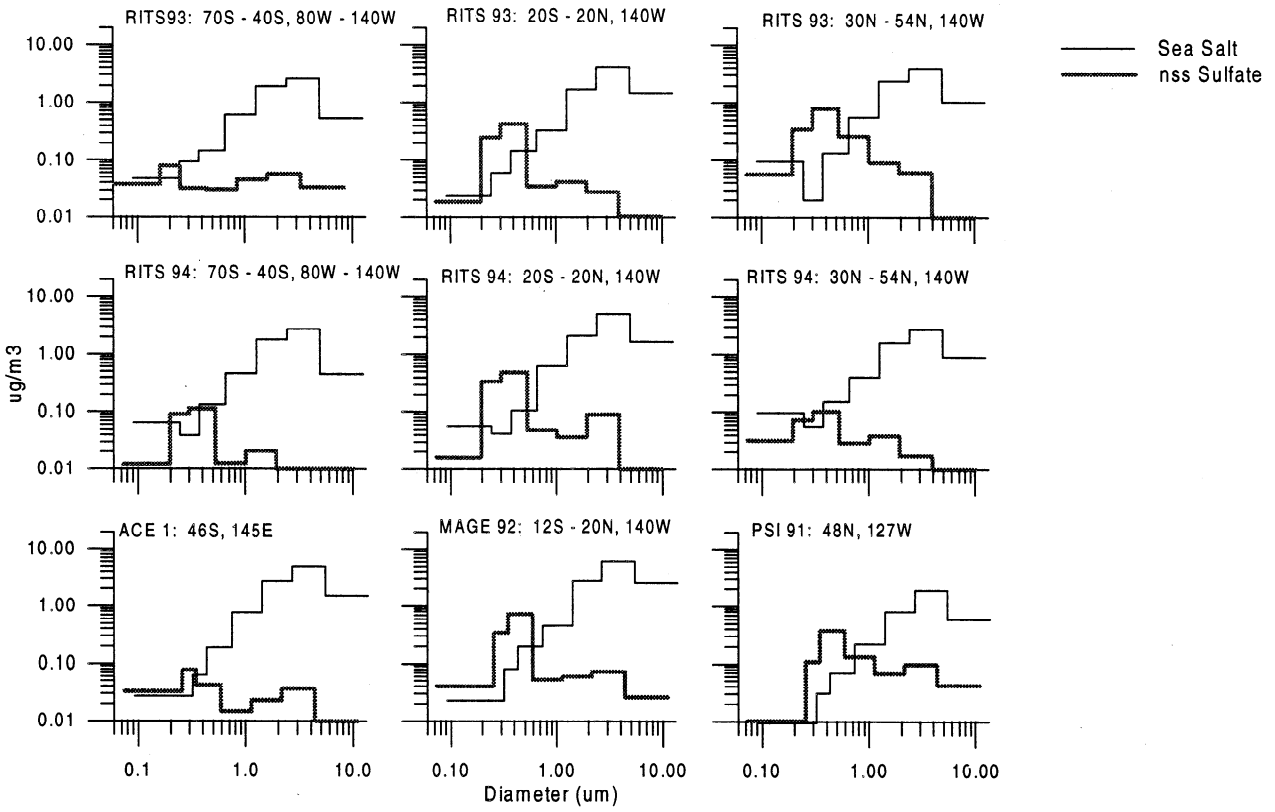

Figure 1. Average sea-salt and nss $SO_4^=$ mass size distributions measured on five cruises throughout the Pacific and Southern Oceans. Data are shown as a function of geometric mass diameter at 70% RH. The RITS 93 and 94 data are segregated into the latitudinal bins considered by *Tegen et al.* [1997].

Table 1. Sea Salt and Nss Sulfate at a Variety of Marine Locations for Two Different Size Ranges: Particles With Geometric Mass Diameters Less Than or Equal to 1.4 μm at 70% RH and Particles With Geometric Mass Diameters Greater Than 1.4 μm and Less Than the Upper Size Cut of the Aerosol Sampling Inlet ($\sim$10 μm)

		Sea Salt $\mu g\ m^{-3}$		Nss Sulfate $\mu g\ m^{-3}$	
	Location	$D \leq 1.4\ \mu m$[a]	$D > 1.4\ \mu m$[b]	$D \leq 1.4\ \mu m$[a]	$D > 1.4\ \mu m$[b]
RITS 93[c]	70°S–40°S, 80°W–140°W	0.84 ± 0.64	4.8 ± 2.3	0.17 ± 0.11	0.13 ± 0.13
	20°S–20°N, 140°W	0.56 ± 0.50	7.4 ± 3.8	0.71 ± 0.49	0.07 ± 0.04
	30°N–54°N, 140°W	0.84 ± 0.96	7.3 ± 4.6	0.99 ± 0.89	0.12 ± 0.08
RITS 94[c]	70°S–40°S, 140°W	0.70 ± 0.31	5.0 ± 2.0	0.23 ± 0.13	0.03 ± 0.03
	20°S–20°N, 140°W	0.82 ± 0.90	8.8 ± 2.6	0.85 ± 0.47	0.13 ± 0.24
	30°N–54°N, 140°W	0.71 ± 0.15	5.3 ± 2.5	0.24 ± 0.11	0.06 ± 0.03
MAGE 92[d]	12°S–20°N, 140°W	0.75 ± 0.55	12 ± 6.0	1.0 ± 0.67	0.16 ± 0.21
PSI 91[d]	48°N, 110°W	0.33 ± 0.29	3.3 ± 2.3	0.63 ± 0.35	0.21 ± 0.16
ACE 1[e]	46°S, 145°E	1.0 ± 0.56	9.3 ± 5.4	0.17 ± 0.06	0.07 ± 0.09

[a]The 1.4 μm is an operational division based on the 50% cutoff diameter of the impactor jet plate.
[b]Size range extends to the upper size cut of the aerosol sampling inlet ($\sim$10 μm).
[c]*Quinn et al.* [1996].
[d]*Quinn et al.* [1995].
[e]*Quinn et al.* [1998].

coastal regions (0.33 ± 0.29 $\mu g\ m^{-3}$ during PSI 91). In contrast, nss $SO_4^=$ concentrations in this size range are much more variable (0.56 ± 0.36 $\mu g\ m^{-3}$) as they depend on highly variable local sources, transport of air from continental regions, and the amount of time the aerosol spends in the boundary layer prior to removal by rain [*Quinn et al.*, 1996; *Covert et al.*, 1996]. A lengthy boundary layer residence time allows for the accumulation of sulfate mass via the cycling of aerosol through nonprecipitating clouds and the heterogeneous deposition of gas phase species [*Hoppel et al.*, 1994]. The ratio of sea salt to nss $SO_4^=$ in this size fraction ranges from 0.52 to 6.2. In general, the highest ratios are found in the high southern latitudes remote from continental sources of sulfate aerosol. An exception to this is RITS 94 in the 30°N to 54°N region where low sulfate concentrations were measured corresponding to marine air advecting from the northwest [*Quinn et al.*, 1996]. Clearly, over widespread regions of the Pacific atmosphere, sea salt is the dominant component of submicron aerosol.

As expected, based on the different production mechanisms of sea salt and nss $SO_4^=$ (wind-driven mechanical production versus heterogeneous reactions, respectively), sea-salt concentrations in the size range $1.4 < D < 10$ μm dominate those of nss $SO_4^=$.

To calculate the global distribution of sea salt, *Tegen et al.* [1997] start with an exponential relationship between surface wind speed and sea-salt mass concentration following the method of *Erickson et al.* [1986]

$$m_{\text{sea salt}} = e^{0.16u+1.45} \quad (u < 15\ \text{m s}^{-1}) \qquad (1)$$

$$m_{\text{sea salt}} = e^{0.13u+1.89} \quad (u > 15\ \text{m s}^{-1}) \qquad (2)$$

where $m_{\text{sea salt}}$ is the mass concentration in $\mu g\ m^{-3}$, and u is surface wind speed. The relationship for $u <$ 15 m s^{-1} is based on empirical data of *Lovett* [1978]. For comparison, we apply the same log linear relationship to the local wind speeds and concentrations measured during the RITS, MAGE, PSI, and ACE cruises. The resulting values of the slope, y intercept, and coefficient of determination of the regression are shown in Table 2. The range of values of the slope encompasses the values used by *Tegen et al.* [1997] (0.13 to 0.22 for $D \leq 1.4$ μm and 0.1 to 0.4 for $D > 1.4$ μm versus 0.16) and agrees, in general, with values reported for a variety of oceanic regions [e.g., *Gong et al.*, 1997; *Gras and Ayers*, 1983]. These data cannot be used to compare with the relationship employed by *Tegen et al.* [1997] for $u >$ 15 m s^{-1} as wind speeds this high were not encountered over the course of an entire impactor sampling period.

The rather low r^2 values imply that only a portion of the variance in the sea-salt mass concentration can be explained by the local wind speed. The lifetime of up to a couple days associated with the measured size range ($D < 10$ μm) results in the influence of other factors on the mass concentration, including advection and vertical mixing. Hence an accurate description of the size-dependent concentration of sea salt throughout the boundary layer requires a more sophisticated transport model than a simple regression between locally measured surface wind speed and sea-salt mass concentration [*Bates et al.*, 1998; *Quinn et al.*, 1998]. A more fitting role for shipboard observations of sea salt is the validation of the lower-altitude size distributions calculated by the transport model.

4. Scattering Due to Sea Salt

Assuming an externally mixed aerosol composed of nss $SO_4^=$ (which includes nss $SO_4^=$ plus associated NH_4^+) and sea salt, Mie scattering theory was used to parti-

Table 2. Results of a Log-Linear Fit of the Form $m_{\text{sea salt}} = e^{au+b}$ (Equation (1)) of the sea-salt Mass Concentration ($m_{\text{sea salt}}$) and Local Wind Speed (u) Measured at a Height of 10–18 m ASL

	Location	Average Wind Speed, u m s^{-1}	$D \leq 1.4$ μm			$1.4 < D < 10$ μm		
			a	b	r^2	a	b	r^2
RITS 93/94[a]	70°S–40°S, 80°W–140°W	11 ± 2.0	0.20	−2.6	0.34	0.13	−0.02	0.34
RITS 93/94 and MAGE[a,b]	20°S–20°N, 140°W	8.5 ± 2.7	0.12	−1.5	0.20	0.11	1.1	0.35
RITS 93/94[a]	30°N–54°N, 140°W	10 ± 3.7	0.21	−2.7	0.78	0.10	0.79	0.41
PSI 91[b]	48°N, 110°W	6.0 ± 1.6	0.22	−2.7	0.20	0.40	−1.6	0.66
ACE 1[c]	46°S, 145°E	9.0 ± 2.4	0.13	−0.92	0.42	0.14	1.1	0.41

ASL, above sea level. The fit was performed on two size ranges: $D \leq 1.4$ μm and $1.4 < D < 10$ μm, where D is the geometric mass diameter at 70% RH. For comparison, the relationship used by *Tegen et al.* [1997] for $u < 15$ m s^{-1} employed a value of $a = 0.16$. Also shown is the coefficient of determination of the regression r^2.

[a] *Quinn et al.* [1996].
[b] *Quinn et al.* [1995].
[c] *Quinn et al.* [1998].

tion measured scattering coefficients among nss $SO_4^=$ aerosol, submicron sea salt ($D \leq 1.0$ μm at 30 to 40% RH), and supermicron sea salt ($1.0 < D < 10$ μm at 30 to 40% RH) [*Quinn et al.*, 1995, 1996, 1998]. The scattering calculations were performed at the low reference RH of 30 to 40% to allow for a direct comparison to the scattering coefficients measured at the same reference RH. Measured size distributions of the aerosol number concentration and nss $SO_4^=$ and sea-salt aerosol mass concentrations were used as input data. The assumption of an aerosol composed only of sea salt and nss $SO_4^=$ is supported by mass closure measurements which indicate that only a small fraction of the submicron mass is composed of other chemical species (14 ± 15% for ACE 1 and RITS 93/94, 20 ± 15% for MAGE 92, and 40 ± 15% for PSI 91). The assumption will lead to an overestimation of submicron scattering due to sulfate and/or sea salt, however, scaled to the fraction of "residual" mass present. For all regions surveyed, essentially all of the supermicron mass (>95%) was composed of sea salt with a minor contribution by nss $SO_4^=$.

Average scattering coefficients calculated for each chemical component j, $\sigma_{sp,j}$, are shown in Figure 2 as a function of latitudinal region. The percent of the measured scattering due to each component at 30 to 40% RH is listed in Table 3. The fraction due to submicron plus supermicron sea-salt ranges from 63 to 97%. Of this, 23 to 42% is due to submicron sea salt.

The large fraction of scattering due to submicron sea salt is the result of a high mass-scattering efficiency which is comparable to that of nss $SO_4^=$ (see Table 3). Reported values of mass scattering efficiencies for sulfate and sea-salt aerosol vary due to variability in aerosol properties and differences in the measurement techniques and how the mass-scattering efficiency of an aerosol chemical component is defined (see *Quinn et al.* [1996] for a more thorough discussion). Here we define the mass-scattering efficiency of nss $SO_4^=$ as

$$\alpha_{sp,\text{SO}_4\text{\_ion}} = \sigma_{sp,\text{SO}_4\text{\_aer}} / m_{\text{SO}_4\text{\_ion}} \quad (3)$$

where $\sigma_{sp,\text{SO}_4\text{\_aer}}$ is the scattering due to sulfate aerosol which includes $SO_4^=$ and associated NH_4^+ and H_2O mass, and $m_{\text{SO}_4\text{\_ion}}$ is the mass of the sulfate ion. Likewise, the mass-scattering efficiency of submicron sea salt is defined as

$$\alpha_{sp,\text{sub\_sea salt}} = \sigma_{sp,\text{sub\_sea salt}} / m_{\text{sub\_sea salt}} \quad (4)$$

where $\sigma_{sp,\text{sub\_sea salt}}$ includes submicron sea salt and associated water mass, while $m_{\text{sub\_sea salt}}$ represents the submicron sea salt mass with no associated water. Even though the fraction of sea salt found in the submicron size range is up to an order of magnitude less than that found in the supermicron size fraction, it can contribute similarly to the scattering by the aerosol due to a relatively high mass-scattering efficiency.

Values of $\sigma_{sp,j}$ at ambient RH will be different from those at 30 to 40% RH since water uptake by hygroscopic components results in larger mean diameters and lower refractive indices. To test for the sensitivity of $\sigma_{sp,j}$ to an increase in RH, the Mie-scattering calculations were repeated at ambient RH (70 ± 5%) for the RITS 94 samples collected between 20°S and 20°N. The contribution to scattering by submicron sea salt decreased by an average of 10% as some mass shifted into the supermicron size fraction while that due to supermicron sea salt increased. Still, the 17% of total scattering due to submicron sea salt is comparable to that of nss $SO_4^=$ and cannot be discounted given the relatively long lifetime of aerosol in this size range.

To compare to the sea-salt optical depth values calculated by *Tegen et al.* [1997, Figure 3], we have estimated

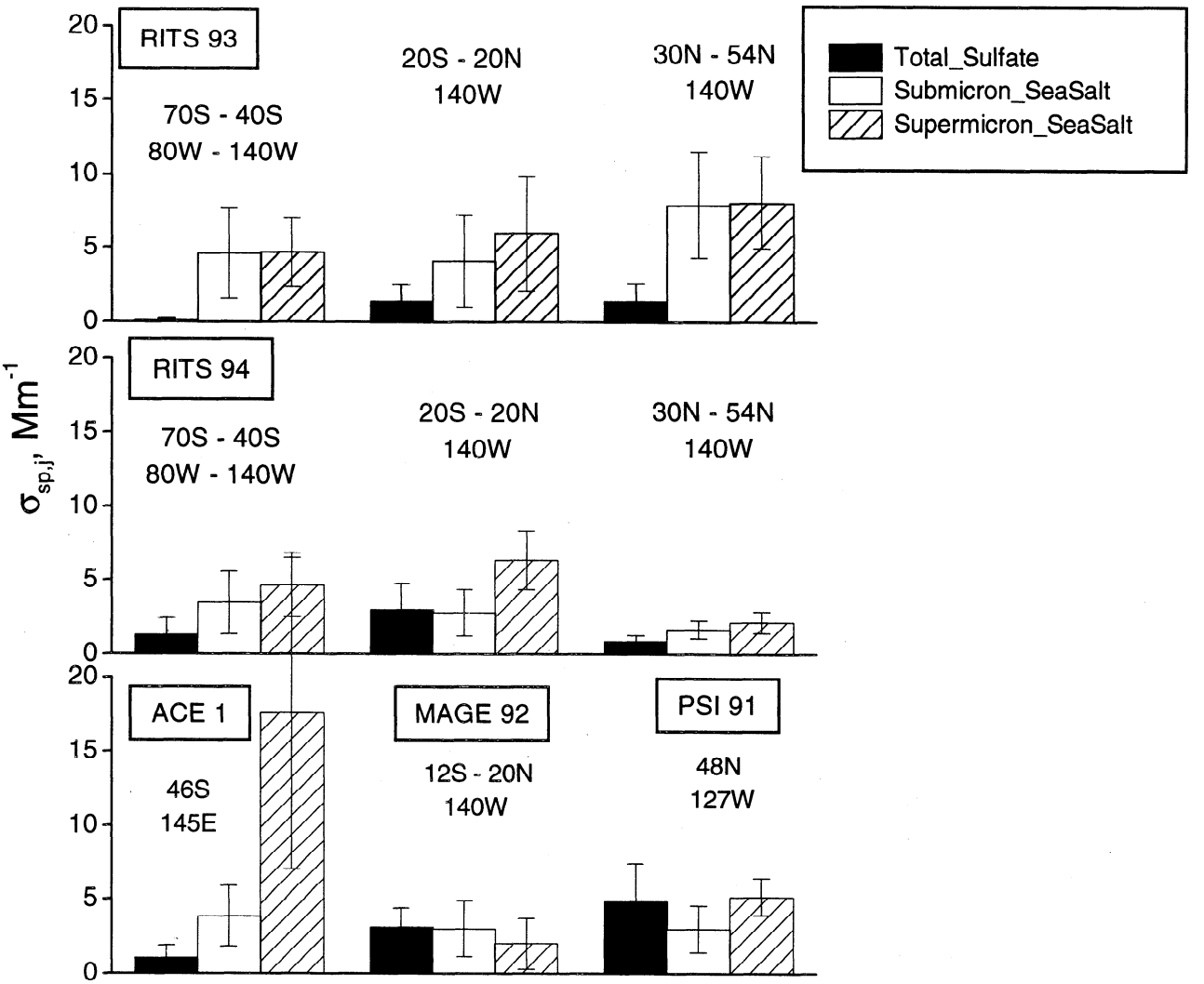

Figure 2. Calculated scattering coefficients $\sigma_{sp,j}$ for nss $SO_4^=$ (includes nss $SO_4^=$ and associated NH_4^+ and H_2O mass for both the submicron and the supermicron size fractions), submicron sea salt, and supermicron sea salt at 30 to 40% RH. Sea salt scattering also includes associated water mass. Values are based on Mie calculations and assume an externally mixed aerosol composed only of nss $SO_4^=$ and sea salt [*Quinn et al.*, 1995, 1996, 1998]. Measured size distributions of the aerosol number concentration and nss $SO_4^=$ and sea-salt aerosol mass concentrations were used as input data. Error bars indicate the standard deviation of the average sample value for each geographical region.

nss $SO_4^=$ and sea-salt optical depths at ambient RH for the RITS 94 tropical samples using

$$\tau_j = \alpha_{sp,j} B_j \quad (5)$$

where τ_j is the optical depth, $\alpha_{sp,j}$ is the mass-scattering efficiency at ambient RH, and B_j is the column burden of chemical component j. B_j is estimated from the mass concentration of j measured at the surface and the MBL height determined from vertical soundings of temperature and dew point. The calculation was done only for the tropics as the MBL is well-defined in this region. Samples collected in the intertropical convergence zone were omitted from the analysis.

Tegen et al. [1997] estimate that sea salt contributes 15 to 22% to the total aerosol optical depth in the latitude band 20°S to 20°N at 140°W. Estimates from the RITS 94 data using equation (5) average 90 ± 10% with 28 ± 15% due to submicron sea salt. Some disagreement is expected due to the neglect of submicron sea salt in the *Tegen et al.* [1997] calculations and the truncation of the measured sea-salt concentrations at 10 μm. Values used for the mass-scattering efficiency of sea salt are another source of discrepancy. *Tegen et al.* [1997] use $\alpha_{sp,j}$ values of 0.2 to 0.4 m^2 g^{-1}. The shipboard measurements indicate that values of 8.7 ± 4.4 m^2 g^{-1} for submicron sea salt and 1.9 ± 0.28 m^2 g^{-1} for supermicron sea salt at 70% RH are more appropriate.

Additional disagreement may result from considering only the MBL in the RITS 94 calculations, which neglects any aerosol layers occurring in the upper tro-

Table 3. Percent of Measured Scattering Due to Nss $SO_4^=$ (Includes Submicron and Supermicron Nss $SO_4^=$ and Associated NH_4^+ and H_2O Mass), Submicron Sea Salt (Includes Sea Salt and Associated H_2O Mass), and Supermicron Sea Salt (Includes Sea Salt and Associated H_2O Mass) for Different Latitudinal Regions

	Percent of Measured Scattering			Percent of Aerosol Optical Depth			Mass-Scattering Efficiency $\alpha_{sp,j}$, $m^2\ g^{-1}$		
	nss $SO_4^=$ $D < 10\ \mu m$	Sea Salt $D \leq 1.0\ \mu m$	Sea Salt $1.0 < D < 10\ \mu m$	Sea Salt[e] $D > 4\ \mu m$	Sea Salt[f] $D \leq 1.0\ \mu m$	Sea Salt[f] $1.0 < D < 10\ \mu m$	nss $SO_4^=$[g] $D < 10\ \mu m$	Sea Salt[h] $D \leq 1.0\ \mu m$	Sea Salt[h] $1.0 < D < 10\ \mu m$
70°S–40°S[a]	7.4 ± 13	42 ± 11	50 ± 9.4	(27)			5.1 ± 0.43	5.5 ± 0.22	0.68 ± 0.08
20°S–20°N[a]	26 ± 12	22 ± 7	52 ± 6		30 ± 8.6	56 ± 6.7	3.0 ± 1.5	4.1 ± 2.1	0.79 ± 0.13
(20°S–20°N[a,b])	(19 ± 10)	(17 ± 11)	(64 ± 6)	(15)	(28 ± 15)	(63 ± 6.8)	(4.0 ± 1.2)	(8.7 ± 4.4)	(1.9 ± 0.28)
30°N–54°N[a]	11 ± 8.7	42 ± 7.1	47 ± 6.8	(15)			7.4 ± 2.1	3.5 ± 0.62	1.1 ± 0.14
48°N, 127°W[c]	37 ± 20	23 ± 11	40 ± 8.3				4.2 ± 0.48	3.7 ± 0.38	0.9 ± 0.07
46°S, 145°E[d]	2.5 ± 2.2	29 ± 3.4	68 ± 3.9				1.3 ± 0.55	4.5 ± 1.1	1.2 ± 0.18

Also shown are estimates from the model of *Tegen et al.* [1997] and the RITS 94 measurements of the percent of aerosol optical depth due to sea salt. Mass-scattering efficiencies based on data presented here for nss sulfate ion, submicron sea salt, and supermicron sea salt are listed as well. Values in parentheses are at ambient RH, while other values in the table are at 30–40% RH.

[a] *Quinn et al.* [1996].

[b] Estimates from RITS 94 data are at the average ambient RH of 70 ± 5% .

[c] *Quinn et al.* [1995].

[d] *Quinn et al.* [1998].

[e] *Tegen et al.* [1997], minimum contribution of absorbing aerosol.

[f] From RITS 94, calculated from equation (5), average MBL height of 1600 m.

[g] Derived from equation (3).

[h] Derived from equation (4).

posphere. Such layers are expected to contain higher concentrations of sulfate than sea salt due to production of sulfate in the outflow regions of convective clouds [*Hegg et al.*, 1990; *Clarke*, 1993; *Perry and Hobbs*, 1994] and the higher sedimentation velocity of supermicron sea salt. Hence if sulfate aerosol layers exist above the marine boundary layer (MBL), equation (5) would overestimate the contribution of sea salt to the total aerosol optical depth.

The total aerosol optical depth estimated for the 20°S to 20°N latitude band from the RITS 94 data averages 0.05 ± 0.02. Values of τ derived from AVHRR observations during the same time period as the RITS 94 measurements average 0.09 ± 0.03 (P. Durkee, personal communication, 1998). In addition, *Tegen et al.* [1997] estimate a value of 0.06 for the March–April time period in the tropical Pacific. The good agreement between the surface- and the satellite-derived values suggests that aerosol layers above the MBL had a minimal contribution to the total aerosol optical depth in the tropics during these cruises. Instead, discrepancy in the sea-salt aerosol optical depth derived from the cruise data and the model appear to be a difference in the partitioning of the total aerosol optical depth between the various chemical components.

5. Conclusions

The data reviewed here show that for the entire central Pacific from 55°N to 70°S, sea salt dominates the aerosol mass concentration in the marine boundary layer with a significant fraction occurring in the submicron size range. As a result, sea salt is a major contributor to scattering by the aerosol in marine regions. Even though supermicron sea salt peaks outside of the size range most efficient for scattering, its mass concentration is sufficient to compensate for the low scattering efficiency. In addition, submicron sea salt is optically significant due to its high scattering efficiency and lifetime that is comparable to nss $SO_4^=$. Clearly, global transport models of sea-salt distributions will be improved by the inclusion of submicron sea salt. In addition, the inclusion of submicron sea salt into coupled chemical transport/radiative transfer models will provide a more accurate estimate of the optical properties of the background marine aerosol.

Acknowledgments. We thank Phil Durkee and Kurt Nielson for providing aerosol optical thicknesses retrieved from AVHRR observations. This research was funded by the aerosol component of NOAA's Climate and Global Change Program. This is NOAA PMEL contribution number 1936 and JISAO contribution number 480.

References

Bates, T. S., V. N. Kapustin, P. K. Quinn, D. S. Covert, D. J. Coffman, C. Mari, P. A. Durkee, W. J. De Bruyn, and E. S. Saltzman, Processes controlling the distribution of aerosol particles in the marine boundary layer during ACE 1, *J. Geophys. Res., 103,* 16,369–16,383, 1998.

Berg, O. H., E. Swietlicki, and R. Krejci, Hygroscopic growth of aerosol particles in the marine boundary layer over the Pacific and Southern Oceans during ACE 1, *J. Geophys. Res., 103,* 16,535–16,545, 1998.

Chin, M., D. J. Jacob, G. M. Gardner, P. A. Spiro, M. Foreman-Fowler, and D. L. Savoie, A global three-dimensional model of tropospheric sulfate, *J. Geophys. Res., 101,* 18,667–18,690, 1996.

Clarke, A. D., Atmospheric nuclei in the Pacific midtroposphere: Their nature, concentration, and evolution, *J. Geophys. Res., 98,* 20,633–20,647, 1993.

Covert, D. S., V. N. Kapustin, T. S. Bates, and P. K. Quinn, Physical properties of marine boundary layer aerosol particles of the mid-Pacific in relation to sources and meteorological transport, *J. Geophys. Res., 101,* 6919–6930, 1996.

Erickson, D. J., J. T. Merrill, and R. A. Duce, Seasonal estimates of global atmospheric sea-salt distributions, *J. Geophys. Res., 91,* 1067–1072, 1986.

Gong, S. L., L. A. Barrie, and J.-P. Blanchet, Modeling sea-salt aerosols in the atmosphere, 1, Model development, *J. Geophys. Res., 102,* 3805–3818, 1997.

Gras, J. L., and G. P. Ayers, Marine aerosol at southern midlatitudes, *J. Geophys. Res., 88,* 10,661–10,666, 1983.

Hegg, D. A., L. F. Radke, and P. V. Hobbs, Particle production associated with marine clouds, *J. Geophys. Res., 95,* 13,917–13,926, 1990.

Holland, H. D., *The Chemistry of the Atmosphere and Oceans,* 109 pp., John Wiley, New York, 1978.

Hoppel, W. A., G. M. Frick, J. W. Fitzgerald, and R. E. Larson, Marine boundary layer measurements of new particle formation and the effects nonprecipitating clouds have on the aerosol size distribution, *J. Geophys. Res., 99,* 14,443–14,459, 1994.

Liousse, C., J. E. Penner, C. Chuang, J. J. Walton, H. Eddleman, and H. Cachier, A global three-dimensional model study of carbonaceous aerosols, *J. Geophys. Res., 101,* 19,411–19,432, 1996.

Lovett, R. F., Quantitative measurement of airborne sea-salt in the North Atlantic, *Tellus, 30,* 358–363, 1978.

McInnes, L. M., P. K. Quinn, D. S. Covert, and T. L. Anderson, Gravimetric analysis, ionic composition, and associated water mass of the marine aerosol, *Atmos. Environ., 30,* 869–884, 1996.

O'Dowd, C. D., M. H. Smith, I. E. Consterdine, and J. A. Lowe, Marine aerosol, sea-salt, and the marine sulfur cycle: A short review, *Atmos. Environ., 31,* 73–80, 1997.

Perry, K. D., and P. V. Hobbs, Further evidence for particle nucleation in clear air adjacent to marine cumulus clouds, *J. Geophys. Res., 99,* 22,803–22,818, 1994.

Quinn, P. K., S. F. Marshall, T. S. Bates, D. S. Covert, and V. N. Kapustin, Comparison of measured and calculated aerosol properties relevant to the direct radiative forcing of tropospheric sulfate aerosol on climate, *J. Geophys. Res., 100,* 8977–8992, 1995.

Quinn, P. K., V. N. Kapustin, T. S. Bates, and D. S. Covert, Chemical and optical properties of marine boundary layer aerosol particles of the mid-Pacific in relation to sources and meteorological transport, *J. Geophys. Res., 101,* 6931–6951, 1996.

Quinn, P. K., D. J. Coffman, V. N. Kapustin, T. S. Bates, and D. S. Covert, Aerosol optical properties in the marine boundary layer during ACE 1 and the underlying chemical and physical aerosol properties, *J. Geophys. Res., 103,* 16,547–16,563, 1998.

Quinn, P. K., and D. J. Coffman, Local closure during ACE 1: Aerosol mass concentration and scattering and backscattering coefficients, *J. Geophys. Res., 103,* 16,575–16,596, 1998.

Tang, I. N., Chemical and size effects of hygroscopic aerosols on light scattering coefficients, *J. Geophys. Res., 101*, 19,245–19,250, 1996.

Tegen, I., and I. Fung, Contribution to the mineral aerosol load from land surface modification, *J. Geophys. Res., 100*, 18,707–18,726, 1995.

Tegen, I., P. Hollrig, M. Chin, I. Fung, D. Jacob, and J. Penner, Contribution of different aerosol species to the global aerosol extinction optical thickness: Estimates from model results, *J. Geophys. Res., 102*, 23,895–23,915, 1997.

P. K. Quinn and D. J. Coffman, NOAA, PMEL, 7600 Sand Point Way NE, Seattle, WA 98115. (e-mail: quinn@pmel.noaa.gov)

(Received January 14, 1998; revised September 9, 1998; accepted September 23, 1998.)